Available online at www.sciencedirect.com
ScienceDirect
ELSEVIER
Earth and Planetary Science Letters xx (2007) xxx–xxx
EPSL
www.elsevier.com/locate/epsl

Ground-coupled acoustic airwaves from Mount St. Helens provide constraints on the May 18, 1980 eruption

Jeffrey B. Johnson [a,*], Stephen D. Malone [b]

[a] Department of Earth and Environmental Science, New Mexico Institute of Mining and Technology, Socorro, NM, United States
[b] Department of Earth and Space Sciences, University of Washington, Seattle, United States

Received 11 October 2006; received in revised form 20 February 2007; accepted 4 March 2007

Editor: R.D. van der Hilst

Abstract

The May 18, 1980 Mount St. Helens eruption perturbed the atmosphere and generated atmosphere-to-ground coupled airwaves, which were recorded on at least 35 seismometers operated by the Pacific Northwest Seismograph Network (PNSN). From 102 distinct travel time picks we identify coherent airwaves crossing Washington State primarily to the north and east of the volcano. The travel time curves provide evidence for both stratospheric refractions (at 200 to 300 km from the volcano) as well as probable thermospheric refractions (at 100 to 350 km). The very few first-hand reports of audible volcano sounds within about 80 km of the volcano coincide with a general absence of ground-coupled acoustic arrivals registered within about 100 km and are attributed to upward refraction of sound waves. From the coherent refracted airwave arrivals, we identify at least four distinct sources which we infer to originate 10 s, 114 s, ~180 s and 319 s after the onset of an 8:32:11 PDT landslide. The first of these sources is attributed to resultant depressurization and explosion of the cryptodome. Most of the subsequent arrivals also appear to be coincident with a source located at or near the presumed volcanic conduit, but at least one of the later arrivals suggests an epicenter displaced about 9 km to the northwest of the vent. This dislocation is compatible with the direction of the sector collapse and lateral blast. We speculate that this concussion corresponds to a northern explosion event associated with hot cryptodome entering the Toutle River Valley.

Keywords: acoustic airwaves; ground-coupled seismicity; Mount St. Helens

1. Introduction

Mount St. Helens (MSH) erupted spectacularly on the morning of May 18, 1980 following an 8:32:11 PDT magnitude M_l 5.1 earthquake and consequent large landslide/sector collapse onset, which was observed approximately 10 s later [40]. This northward-directed avalanche induced an abrupt unloading of a pressurized magmatic system (e.g., [22,6]), which led to the onset of a vertical eruption column at ~8:32:47 PDT, northward-directed lateral blast at ~8:32:56 PDT, and Plinian phase, which initiated at approximately 8:37:00 PDT [40]. According to satellite imagery [20] convective plume rise then alternated with repeated column collapse and associated co-ignimbrite ash columns for more than 8 h. Because clouds and plume effectively obscured much of the vent and northern flanks of the

* Corresponding author. Tel.: +1 603 862 0711; fax: +1 603 862 2649.
E-mail addresses: jeff.johnson@unh.edu (J.B. Johnson), steve@ess.washington.edu (S.D. Malone).

0012-821X/$ - see front matter © 2007 Published by Elsevier B.V.
doi:10.1016/j.epsl.2007.03.001

volcano starting only a few tens of seconds after the initial eruption onset, visual identification of subsequent explosive pulses was inhibited [19]. Nevertheless, based upon analysis of seismic records [21,26], and photographic and satellite imagery [27,36], there is evidence to support at least two explosive pulses within the first minutes of the initial 8:32:11 PDT earthquake. Due to the complex and extended-duration source processes and saturation of proximal seismographs the identification of individual eruptive phases has been somewhat difficult to constrain seismically. As a result, the time history of potential eruptive pulses at the onset of the MSH paroxysm is not well determined. In an attempt to better understand the eruptive chronology during the first ~5 min of the eruption, we focus here on the analysis of acoustic airwaves recorded on regional seismometers 15 to 32 min after the initiation of the eruption.

First-hand reports gathered from the general public offer some potential insight into the nature of airwaves produced on the morning of May 18, 1980. More than 1200 people responded to a poll that asked for their observations on the audibility of the climactic MSH eruption [9]. With only a few exceptions, mapped reports of audible sound indicate a pronounced zone of silence that extended from as close as 10 km from the volcano to as far as 80 km. At greater offsets, observers cite variations on "a 15 minute barrage of sonic booms, thunder, and dynamiting." [9]. Other observers report "low-frequency concussions, ear-popping, and faint sonic booms" that suggest low-frequencies and/or near-infrasound (<20 Hz) pressure disturbances. Though the eruption remained audible at distances as far as 750 km, well into Montana, California, and British Colombia, the greatest "zone of loudness" was reported at about 200 km with a possible second zone of loudness identified at farther offsets [9]. The alternating zones of sound intensity are qualitative, but hint at first and second refracted arrivals from ray paths turning in the high-velocity stratosphere or thermosphere [9]. These atmospheric refractions are common for acoustic waves ducted in the atmosphere and have been observed during

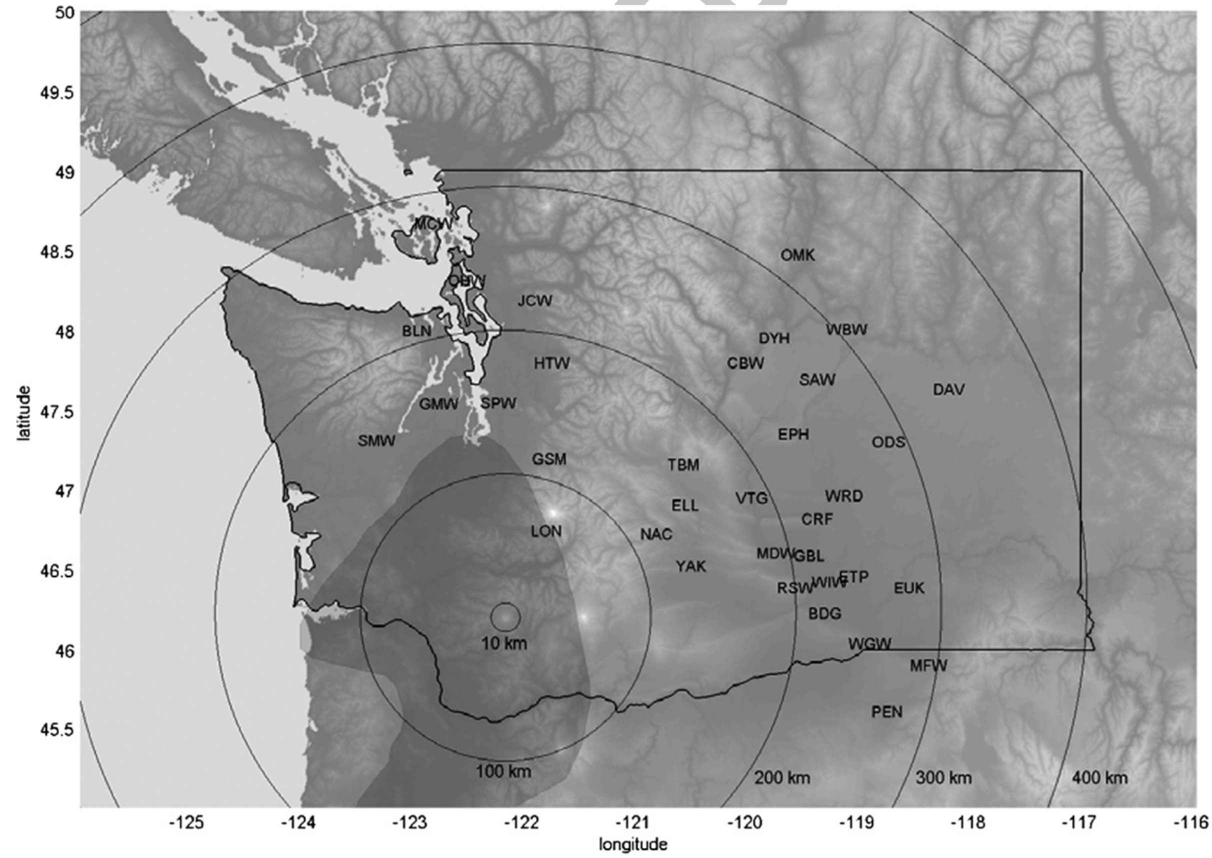

Fig. 1. Map of the 35 PNSN seismic stations that recorded acoustic airwaves from the May 18, 1980 MSH blast(s). Approximate zone of inaudibility is indicated as dark shaded region and comes from Fairfield [9].

Please cite this article as: J.B. Johnson, S.D. Malone, Ground-coupled acoustic airwaves from Mount St. Helens provide constraints on the May 18, 1980 eruption, Earth Planet. Sci. Lett. (2007), doi:10.1016/j.epsl.2007.03.001

high-energy explosive testing [e.g., [2]], as well as during other volcanic eruptions such as Krakatau, Pinatubo, and Pavlov (e.g., [28,38,39]).

2. Data: MSH airwaves recorded by seismometers

Regional seismic data provided a comprehensive record of the May 18 MSH eruptive activity because they responded to the relatively energetic ground-coupled pressure perturbations radiated by the volcano into the atmosphere. In 1980 the Pacific Northwest Seismograph Network (PNSN) operated 72 seismographs distributed throughout Washington and into parts of northeastern Oregon. A subset of 35 of these stations, located primarily to the north and east of MSH, recorded clear airwaves associated with the May 1980 eruption (Fig. 1). As these recordings were made during the dawn of the digital seismic age, data was recorded on a mixture of digital and hard copy media.

Due to the relatively slow propagation speed of sound in the atmosphere (relative to seismic waves in the ground), much of the ground-coupled acoustic arrivals reached the regional seismic network long after the primary seismic shaking associated with the M_l 5.1 earthquake had dissipated. This enabled us to identify robust ground-coupled airwave arrivals on seismograms at instruments located ~67 to 340 km from the source (see examples in Fig. 2). Unfortunately, because the atmosphere-to-ground transmission is so complex, influenced by incidence angle, signal amplitude, site response, and acoustic frequency, we are reluctant to utilize seismic trace characteristics to recover details about the original sound intensity or frequency content of the airwave. It is not possible, for instance, to distinguish whether these records originate from infrasonic (<20 Hz) or sonic waves impinging upon the earth, or alternatively, by mass flow along the ground/atmosphere interface (e.g., caused by abrupt

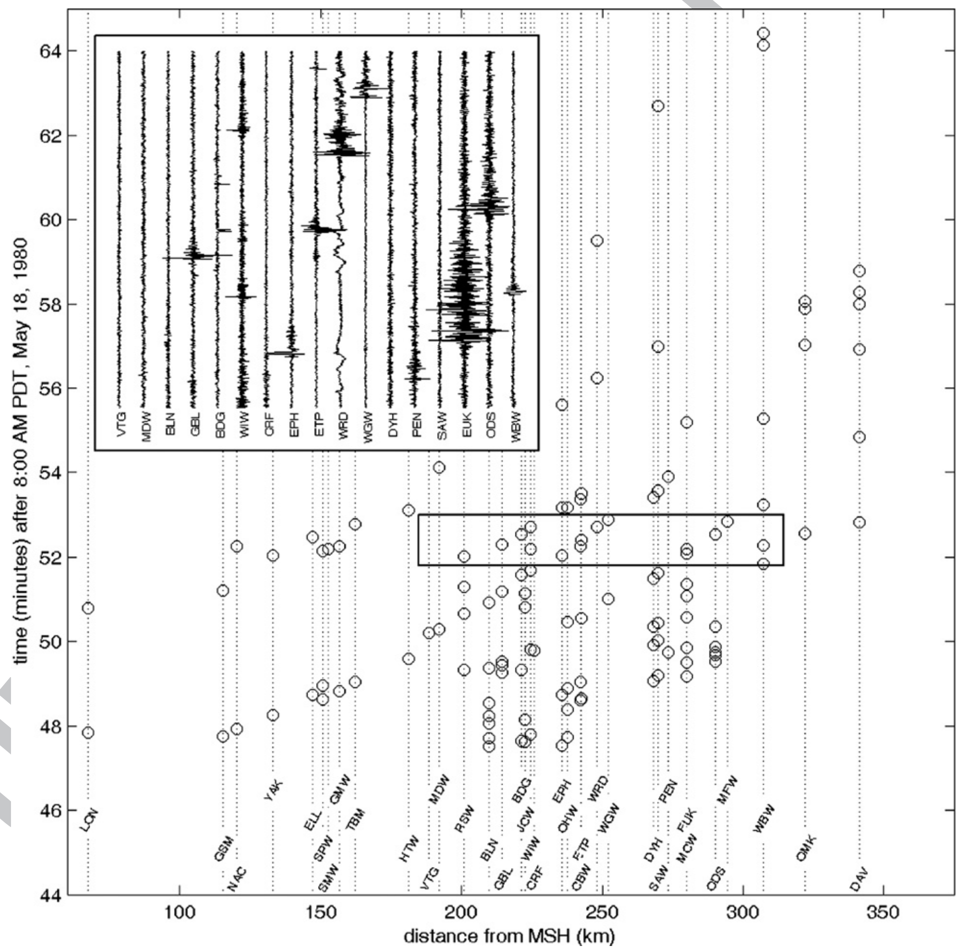

Fig. 2. Complete set of 102 picked airwave arrivals at all 35 stations. Inset panel shows one-minute example velocity seismograms from 17 select short-period seismic stations.

Please cite this article as: J.B. Johnson, S.D. Malone, Ground-coupled acoustic airwaves from Mount St. Helens provide constraints on the May 18, 1980 eruption, Earth Planet. Sci. Lett. (2007), doi:10.1016/j.epsl.2007.03.001

barometric changes or wind), or potentially by other types of seismo-acoustic phases (e.g., ground-coupled Rayleigh waves [24]).

Our analysis of ground-coupled airwaves begins with handpicked arrival times identified on 35 seismographs located 67 to 340 km from the volcano and encompassing an azimuthal distribution of −35° to +103° (relative to north). Between 8:47:18 and 8:56:07 PDT a total of 102 distinct arrivals are identified from digital and paper records with as many as 7 arrivals picked from certain individual stations (e.g., BLN; see Fig. 2). After 8:56:07 PDT a few additional transients were identified at individual stations, but none of these were linked to arrivals at neighboring stations so their significance is unclear. Although we possess no evidence for airwaves arriving prior to 8:47:18 PDT it should be noted that this record could potentially be incomplete. In May 1980 some seismograms were recorded only on digital media following automated earthquake triggering, which may not have occurred for small or isolated ground-coupled airwaves. Although continuous film records were scanned for additional arrivals, only a subset of stations were available from this medium.

Arrival picks may be viewed in a time–distance fashion to identify logically connected “coherent” arrivals propagating across the network. We interpret 91 of the picked arrivals as belonging to nine distinct acoustic travel time (or arrival) curves based upon a reasonable move-out (Fig. 3). The nine coherent airwave travel time curves are separated into three distinct families based upon their apparent velocity. Two arrivals, with apparent velocities of 501 and 520 m/s, are found at close offsets (100 to 200 km). Three arrivals, with very consistent apparent velocities of 334 to 337 m/s, are identified at distances greater than 180 km. And at least four arrivals, with apparent velocities between 371 and 452 m/s, are also found at these greater offsets. Finally, two additional isolated arrivals at extremely close offsets are identified at the seismic station LON, 67 km from MSH.

We are confident in the Fig. 3 travel times curves, which are identified by examining how individual arrivals belong to a single coherent move-out. A linear regression is then applied to the arrivals to establish a slope, which is inversely proportional to the apparent velocity. In a few cases arrivals occur in quick succession (within ∼20 s of one another; e.g., station

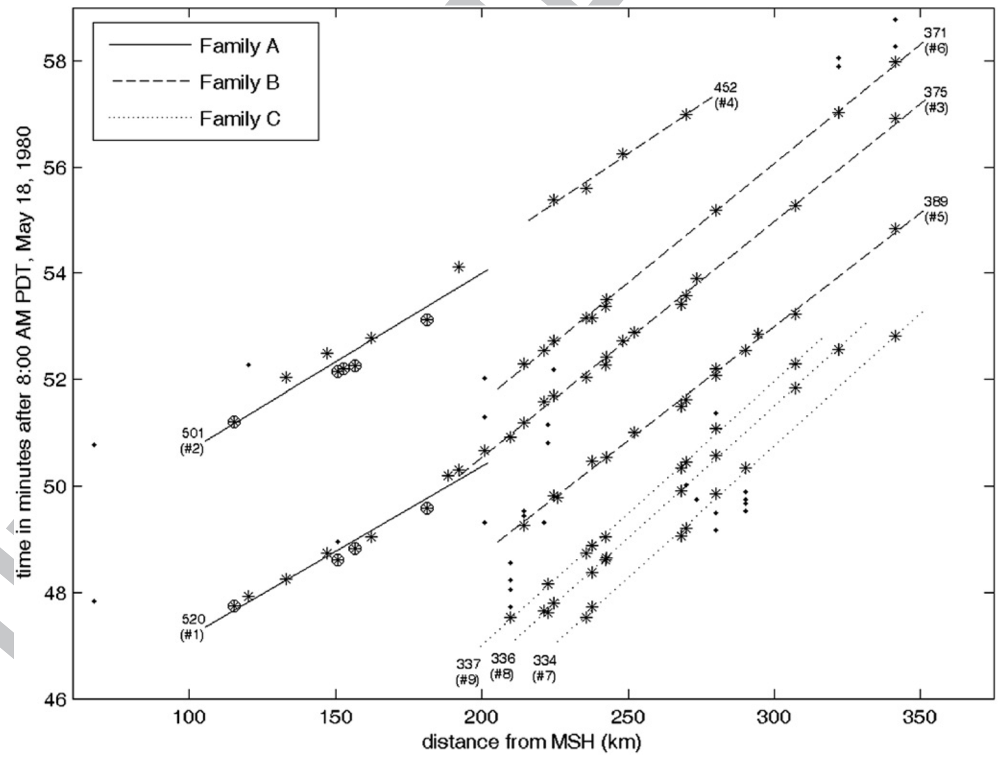

Fig. 3. Primary travel time curve interpretation for MSH ground-coupled arrivals. For each curve the apparent velocity and an arrival curve reference number are indicated (in brackets). Asterisks (⁎) indicate the picks used in arrival curve linear regression fits. Small circles (·) indicate additional picks not easily attributed to any coherent travel time move-out. Encircled asterisks in arrivals #1/2 indicate stations located primarily to the north of MSH.

Please cite this article as: J.B. Johnson, S.D. Malone, Ground-coupled acoustic airwaves from Mount St. Helens provide constraints on the May 18, 1980 eruption, Earth Planet. Sci. Lett. (2007), doi:10.1016/j.epsl.2007.03.001

BLN) and their inclusion or exclusion in a particular curve is a judgment decision based upon a best fit with arrivals at similar offsets. Single erroneous picks may modestly affect the apparent velocity of an arrival; for instance, incorporation of the second BLN arrival would change the apparent velocity of the corresponding curve by +13 m/s. Overlapping travel time curves with different slopes are not identified in our data. In a few instances we have discounted an arrival that did not easily fit into any specific travel time curve. Examples of selective exclusion include the omission of the second arrival at station NAC or the second arrival at station SPW (refer to Fig. 2); some of these 'mispicks' could potentially be explained by ambient noise. In spite of these subjective decisions we are satisfied with the identification of the primary coherent arrivals and the estimation of their approximate apparent velocities. It is notable that all arrival time picks were identified prior to, and independent of, the subsequent ray path modeling presented below.

3. Modeling

Coherent arrivals are analyzed in terms of their apparent velocities to determine their angle of incidence at the earth's surface and turning altitudes. We then employ forward ray path modeling to recover likely atmospheric propagation paths and transit time for refracted energy at different altitudes. The calculated transit times require that multiple source origin times (i.e., multiple events) be invoked to explain the multiple arrivals in the ground-couple seismic data. Based upon minimization of arrival time residuals we demonstrate that at least one of the later travel time curves should be attributed to a source displaced from the MSH vent region.

3.1. Propagation paths

Recovered apparent velocities c_a provide information about the angle of incidence i with which presumed MSH airwaves are impinging upon the ground (at $z \approx 0$) in the vicinity of the seismographs. Here the angle of incidence is measured in the traditional sense, with respect to a vertical incidence

$$i = \sin^{-1}\left[\frac{c(z \approx 0)}{c_a}\right] \tag{1}$$

and the intrinsic sound speed $c(z)$ in the atmosphere is calculated from virtual acoustic temperature ($c(z) \approx \sqrt{401.87T(z)}$ [11] where $T(z)$ at a specific height is measured in kelvin). To solve for incidence angle at ground level the temperature $c(z \approx 0)$ must be known or estimated. Table 1 displays calculated incidence angles for the nine travel time curves presented in Fig. 3 at a range of temperatures ($T(0)=0$ to 20 °C; 273–293 K). These temperatures encompass a reasonable range of conditions in Washington State in May at elevations below ~2.5 kilometer elevation and at ~9:00 AM in the morning. The nine travel time curves have been separated into three different groupings, or families (i.e., A–C), based upon similar apparent velocities and incidence angles. These families suggest three distinct turning altitudes in a horizontally stratified atmosphere.

Assuming that ray theory is appropriate for our propagating acoustic waves, a ray parameter p may be conserved throughout the ray trajectory in non-moving media [1]. Here we consider that incidence angle, intrinsic sound speed and apparent velocity are functions of altitude z:

$$p = \frac{\sin(i(z)f)}{c(z)} = \frac{(z + r_{\mathrm{Earth}})}{c_a(z)} \tag{2}$$

where r_{Earth} is the earth's radius at $z=0$.

A windless atmosphere is an incomplete approximation of the effective velocity structure. For an atmospheric structure that is radially stratified in terms of temperatures and horizontal winds, a modified ray parameter can be utilized [e.g., from [12]]:

$$p = \frac{(z + r_{\mathrm{Earth}})\sin(i)}{c(z)}\left[1 + \frac{u(z)\sin(i(z))}{c(z)}\right]^{-1} = \frac{(z + r_{\mathrm{Earth}})}{c_a(z) + u(z)} \tag{3}$$

In this case $u(z)$ is the horizontally wind speed in the direction of propagation.

Table 1
Travel time curve number (as displayed in Fig. 3), associated apparent velocity, incidence angles for temperature range, and apparent velocity family grouping based upon similarities in incidence angle

Arrival #	c_a (m/s)	i for $T(0)=0$–20 °C (degrees)	Family
1	520	40–41	A
2	501	41–43	A
3	375	62–66	B
4	452	47–49	B
5	389	58–62	B
6	371	63–68	B
7	334	83–90	C
8	336	81–90	C
9	337	80–90	C

The ray path turning altitude is found for horizontal incidence angles (i.e., $i=90°$). We can thus expect energy to return to earth from altitudes where the following condition is satisfied:

$$c(z)+u(z)\geq\frac{(z+r_{\mathrm{Earth}})}{z}c_{\mathrm{a}}(z=0) \tag{4}$$

At tropospheric to lower thermospheric altitudes (i.e.,< 150 km) the coefficient on the right side of Eq. (4) remains relatively constant and earth curvature effects, in terms of ray path modeling, are found to be relatively insignificant.

Because radiosonde data is limited to a few tens of kilometers altitude, we utilize a COSPAR 1986 International Reference Atmosphere (CIRA) model [10,31] to determine turning altitudes for airwaves propagating into the upper stratosphere and thermosphere. CIRA provides tabulated empirical data for monthly zonal winds and temperatures at 10 degree latitude increments. Fig. 4 shows sample temperature, wind, and calculated turning altitude profiles (both eastward and northward) for several latitudes (40° and 50°) during 3 months (April, May, and June), which are intended to bracket potential conditions for the May 18, 1980 MSH eruption. Because the CIRA data extend to only 120 km, we supplement the temperature profile for higher altitudes with modeled data for May 18th at 46.2° N from the Mass Spectrometer Incoherent Scatter (MSIS 90) model [16,17]. Due to extreme and largely unconstrained, variability of wind data in the thermosphere above 120 km, we fix the zonal winds at 0 m/s and comment on the potential influence of high thermosphere winds in the Discussion section.

The third and fourth profiles of Fig. 4 display an 'effective velocity' (i.e., the lefthand side of Eq. (4)) for both eastward and northward-directed acoustic waves. In the case of northward propagating sound we have set the traditionally less intense meridional winds to zero to highlight extreme variations that might be encountered in the atmosphere. We infer that radiated sound is capable of refracting back to earth where this effective velocity exceeds the various apparent velocities of the different families (C, B, and A) recovered directly from the seismic data. This figure shows the clear capabilities for sound turning in both the stratosphere/mesosphere and thermosphere under a range of atmospheric profiles.

Using a predetermined atmospheric structure it is possible to estimate atmospheric propagation paths using ray tracing [14] and calculate transit times for a known acoustic source at pre-determined altitude [e.g., [8,12,15]]. It is important to consider that the forward modeling requires strong assumptions about the temperature and wind structure up into the thermosphere and that direct measurements in and above the

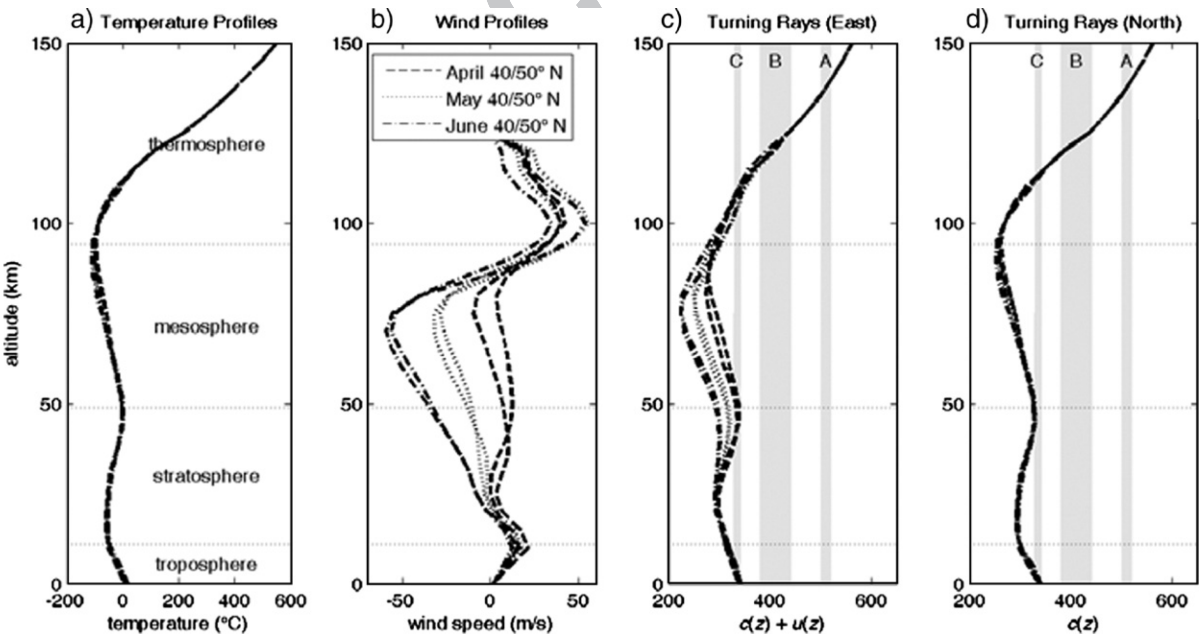

Fig. 4. a) Temperature, b) zonal wind, and c, d) 'effective velocity' (eastwards and northwards) plotted as a function of altitude. Six distinct profiles correspond to April, May, and June profiles for 40 and 50 degree latitudes. Shaded bands in panels c and d correspond to the apparent velocities calculated in Table 1. Band C encompasses the family of arrivals #7–9 and suggests rays turning at the stratopause or lower mesosphere. Bands B and A encompass the family of arrivals #3–6 and #1–2 respectively and suggest rays turning in the thermosphere at altitudes greater than ~120 km.

stratosphere are not available near MSH on May 18, 1980. We are forced instead to rely on empirical models such as MSIS 1990 and COSPAR CIRA 1986 for estimates of horizontally stratified atmospheric conditions. These profiles give average atmospheric structures for a specific latitude and season, but in reality the conditions will vary day to day and during the course of a day. Short-term (hourly) variations may be especially pronounced for winds in the thermosphere above about 150 km [18].

It is uncertain how precisely ray theory can be applied to the atmosphere for the wavelengths in question. Scattering is expected for acoustic waves due to localized wind shear and/or turbulence, which results in extreme temperature gradients over potentially very small distances. Although ray theory is thus not a satisfactory predictor of all the acoustic arrivals commonly observed [e.g., [13]], we apply ray path modeling here to obtain travel time estimates for expected stratospheric/mesospheric and thermospheric refractions. Toward this goal, ray tracing provides valuable insights into regional sound propagation and is computationally simple to perform compared to alternative methods, such as finite difference wave propagation models. Forward modeling is vital and is used in this study for comparison with observed ground-coupled airwave arrival times in order to deduce the source origin time(s) of the various events.

We illustrate projected ray paths from a hypothetical MSH source at 2.5 kilometer elevation according to Eq. (3) (see Fig. 5a). Ray paths are shown for acoustic waves propagated in a zonal (easterly) and meridional (northerly) direction. The zonal propagation uses winds and temperatures from COSPAR CIRA 1986 tables taking the average of the 40 and 50° N May profiles. Above 120 km, MSIS 1990 modeled temperatures for May 18 at 46.2° N, 122° W are utilized. The meridional ray path modeling is performed using an atmosphere with the same temperature profile and no horizontal winds. Though meridional winds in the upper atmosphere are by no means stagnant, they are significantly less than zonal winds. The zero velocity wind field is useful for demonstrating a potential extreme scenario.

The ray tracing is performed by conserving the wind-adjusted ray parameter (p; Eq. (3)) for a range of initial inclinations ranging from 0 to 90 degree incidence. Fig. 5a illustrates a range of conceivable propagation paths in the two orthogonal directions. It is interesting to note that when the ray tracing is performed according to classical ray theory in two dimensions, acoustic energy returns to earth only at very limited distances (<20 km and >250 km). This significant shadow zone offers a convenient explanation for the lack of audible sounds at intermediate distances from the volcano. It is also noteworthy that there is no predicted stratospheric refraction for the modeled eastward propagating acoustic energy. Scattering and three dimensional structure can likely explain how acoustic energy returns to the earth at a much wider range of azimuths and propagation distances than shown in this simplistic ray tracing model, and thus why the observed shadow zone is smaller than predicted.

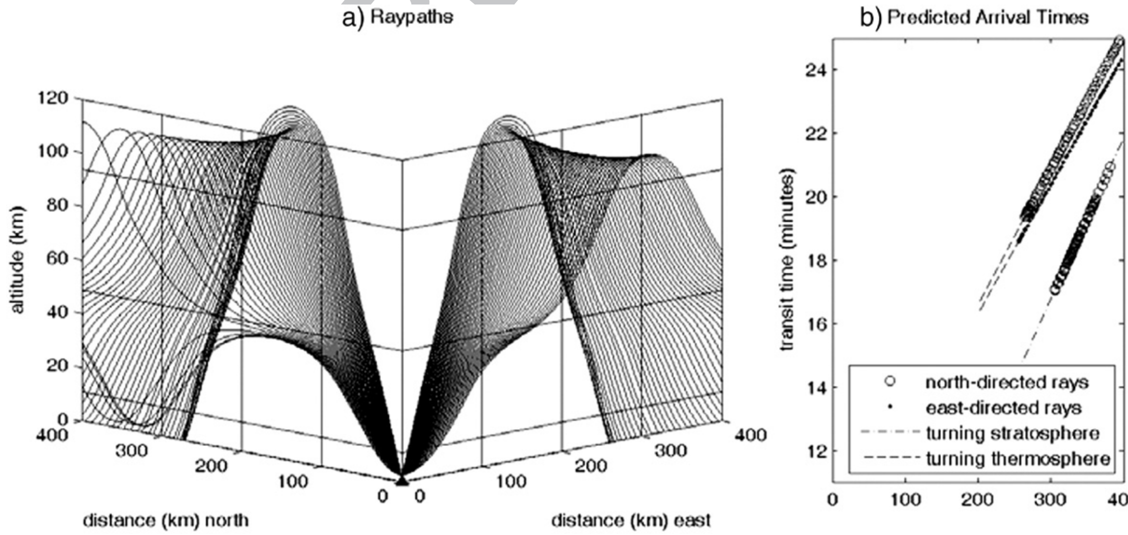

Fig. 5. Ray paths and travel time curves for a MSH acoustic source at 2.5 km elevation. a) Eastward and northward directed ray paths radiated at 1 degree increments. b) Arrival times for rays returning to the ground (<2.5 kilometer altitude) to the east and north. Difference in transit times for thermospheric refractions to the east and north is ~25 s.

Please cite this article as: J.B. Johnson, S.D. Malone, Ground-coupled acoustic airwaves from Mount St. Helens provide constraints on the May 18, 1980 eruption, Earth Planet. Sci. Lett. (2007), doi:10.1016/j.epsl.2007.03.001

3.2. Evidence for multiple sources and source locations

Arrival times from rays with different ray parameters are used to construct synthetic travel time curves for both stratosphere and thermosphere refracted energy (Fig. 5b). These curves can then be compared to the observed arrivals #3–9 (families B and C in Fig. 3) to estimate source origin times for the different observed arrivals. As many as five distinct origin times (i.e., distinct events) are invoked to match the primary observed arrivals (Fig. 6).

Multiple travel time curves with similar slopes and significantly different *y* intercepts point strongly to the existence of multiple sources following an 8:32:11 PDT earthquake. An alternative explanation, multipathing of rays, can not be entirely discounted considering our simplified two dimensional assumptions and modeling. However, we note that even the earliest family of arrivals (family C; arrivals #7–9), which occur in quickest succession, are separated by 75 s. If these arrivals were due to a single source time, the arrival time difference must be explained by transit distances, which would vary by about 25 km and which would require turning altitudes that vary by many tens of kilometers. For ray path modeling in a typically stratified atmosphere we would not expect turning altitudes to have such an exaggerated range for a single ray parameter value.

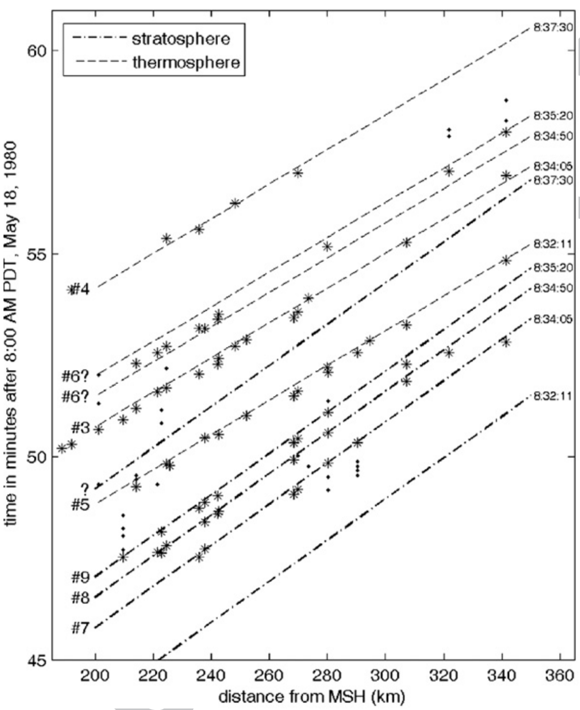

Fig. 6. Modeled acoustic arrivals (at 200–350 km) for northward-directed refraction in the thermosphere and stratosphere for five hypothetical MSH sources occurring at 8:32:11, 8:34:05, 8:34:50, 8:35:20, and 8:37:30 PDT. Source origin times have been picked to best coincide with observed arrivals #3–9 (annotated at left side of plot). A summary of speculated source mechanisms for the five source events is summarized in Table 3 and presented as a timeline in Fig. 8.

Assuming that arrivals at a specific offset and with similar observed apparent velocities are due to multiple sources, we identify three distinct arrivals corresponding to stratosphere refractions, two arrivals corresponding to thermosphere refractions at near-offsets (less than 200 km) and four distinct arrivals corresponding to thermosphere refractions at greater offsets (beyond 200 km). The earliest source associated with any of the travel time curves is identified as a thermosphere refraction (arrival #5), which points to an origin time shortly after 8:32:11 PDT. A corresponding stratosphere refraction that might be associated with this original event is notably absent in our data.

Although an accompanying stratosphere refraction is not evident for the first thermosphere refraction, the second thermosphere refraction (arrival #3) appears associated with the first definitive stratosphere refraction (arrival #7). This source would correspond to an event occurring at 8:34:05 PDT approximately 114 s after the earthquake, and based upon analysis of travel time differences (see below), is likely associated with arrival #1, which is recorded at closer offsets.

A subsequent thermosphere refraction (arrival #6) may be associated with either one (or both) of the stratosphere refractions #8/9, which occur in relatively rapid succession and are inferred to have source origin times at 8:34:50 PDT and 8:35:20 PDT (159 s and 189 s after the original earthquake). There is no clearly distinguishable stratosphere refracted travel time curve corresponding to the last thermosphere refraction (arrival #4), which is inferred to have an 8:37:30 source origin time (319 s after the original event). Arrival #4 appears as a continuation of, and is likely associated with, arrival #2 recorded at near offsets.

Of the four thermosphere refracted travel time curves that are identified at further offsets, two of them (arrivals #3/4) appear to be associated with the travel time curves identified at closer offsets (arrivals #1/2). This conclusion is based upon the continuous nature of their line segments (refer to Fig. 3) and the consistent ΔT_{2-1} time differences, which are similar to the ΔT_{4-3} time differences (see Table 2). These two distinct sources appear to radiate coherent airwaves that can be traced from 110 to 340 km from the volcano. From Table 2, we further note evidence for consistent time differences

Please cite this article as: J.B. Johnson, S.D. Malone, Ground-coupled acoustic airwaves from Mount St. Helens provide constraints on the May 18, 1980 eruption, Earth Planet. Sci. Lett. (2007), doi:10.1016/j.epsl.2007.03.001

Table 2
Time differences (ΔT_{y-x}) between select arrivals at individual stations y and x

	ΔT_{2-1}		ΔT_{6-5}		ΔT_{9-8}	ΔT_{9-7}
(GSM)	208	GBL	182	JCW	32	
YAK	227	WIW	174	EPH		72
ELL	225	OHW	162	OHW	30	69
(SPW)	212	ETP	177	CBW	26	
(GMW)	205	EUK	179	DYH	26	77
TBM	225	DAV	189	SAW		75
(HTW)	212	Mean	177	MCW	30	74
MDW	229	SD	9.0 s	WBW	26	
Mean	218			Mean	28	73
SD	9.6 s			SD	2.7 s	3.0 s
	ΔT_{4-3}		ΔT_{LON}			
WIW	221	LON	177			
EPH	214					
WRD	212	$\Delta T_{2-1} \approx \Delta T_{4-3}$				
SAW	205					
Mean	213	$\Delta T_{6-5} \approx \Delta T_{LON}$				
SD	6.6 s					

For arrivals #1/2, the stations located to the north are highlighted in parentheses. Mean and standard deviation time differences are provided for each station grouping.

between arrivals #5/6 (ΔT_{6-5}; mean = 177 s) and the time difference (also 177 s) between the ground-coupled phases identified at seismograph LON (67 km from MSH). Furthermore, we justify our identification of three distinct stratosphere refractions as corresponding to three separate sources based upon consistent time delays (ΔT_{9-8} and ΔT_{9-7}). A few other ground-coupled arrivals identified prior to arrival #7 hint at potential additional sources, but not enough stations are picked to clearly define additional travel time curves prior to arrival #7.

For arrivals #1/2 we note a systematic difference between ΔT_{2-1} for stations located to the north (mean 209 s; standard deviation 3.4 s) and stations located to the east (mean 226.5 s; standard deviation 1.9 s). If atmospheric structure remains unchanged during this ~3.5 minute interval, this systematic difference can be attributed to a displacement in source location for the second event relative to the first event. To first order, the second source should be ~17 s closer to northern stations than to eastern stations. Utilizing the average apparent velocity of the two arrivals in family A ($c_{a(A)}$ = 510 m/s), it appears that the second source should be ~9 km closer to the northerly stations than to the easterly stations.

To more precisely constrain the source region responsible for arrival #2, we performed a 2-D grid search of possible epicenters assuming that the first source corresponds to the MSH vent/conduit/summit. We then attempted to minimize root mean squared time residuals (T_{RMS}), which are based upon differences between the observed (ΔT_{2-1}) and expected ($\Delta T_{Expected}$) arrival times differences at $n = 8$ stations:

$$T_{RMS} = \sqrt{\sum_{sta=1}^{n} \left(\Delta T_{2-1}(sta) - \Delta T_{Expected}(sta)\right)^2 / n} \tag{5}$$

where for all stations:

$$\Delta T_{Expected}(sta) = \frac{D_{vent}(sta) - D_{loc}(sta)}{c_{a(A)}} - \left(\frac{1}{n}\sum_{i=1}^{n} \Delta T_{2-1}(i) + \frac{D_{vent}(i) - D_{loc}(i)}{c_{a(A)}}\right) \tag{6}$$

Here D_{vent} is the horizontal distance between the MSH vent and each seismic station, D_{loc} is the distance between grid search location and each seismic station, and ΔT_{2-1} is the observed time differences between arrivals #1/2. Each of these three values is station dependent. Calculations are made for a source zone that is assumed to be small (i.e., a point source) and neglects potential source elevation variations, which are a minor influence. In this manner the source location with smallest T_{RMS} can be mapped (see Fig. 7).

Assuming arrival #1 corresponds to the MSH vent, arrival #2 presents a very large residual for both a subsequent MSH vent source (T_{RMS} = 9 s) as well as for a hypothesized Spirit Lake epicenter (T_{RMS} = 8 s)

Please cite this article as: J.B. Johnson, S.D. Malone, Ground-coupled acoustic airwaves from Mount St. Helens provide constraints on the May 18, 1980 eruption, Earth Planet. Sci. Lett. (2007), doi:10.1016/j.epsl.2007.03.001

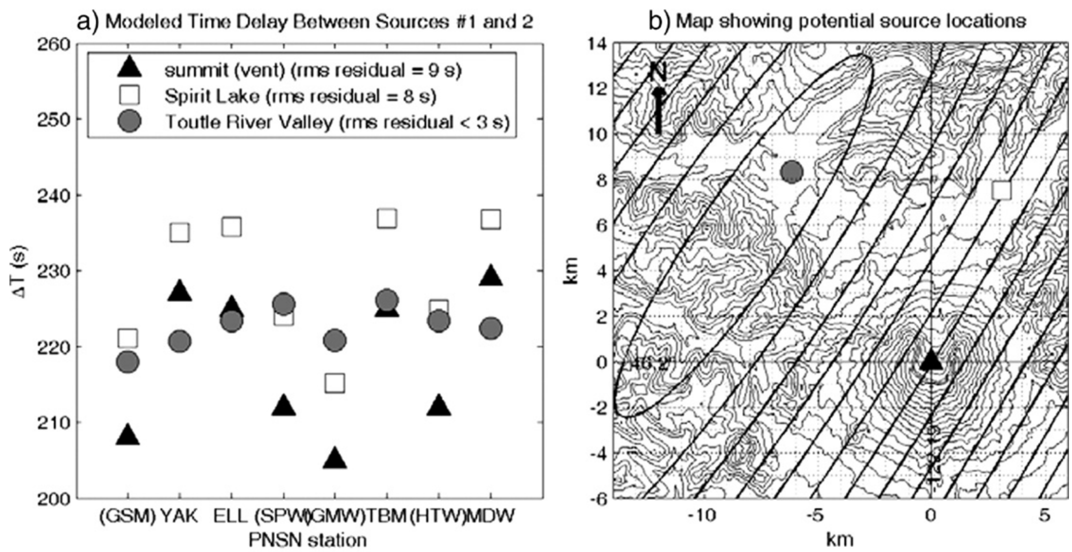

Fig. 7. Time residuals and candidate source locations for arrival #2. a) Expected time differences for ΔT_{2-1} for three candidate subsequent source regions (MSH vent, Spirit Lake, and Toutle River drainage). The four stations located to the north are identified with brackets, e.g., (GSM). The average ΔT_{2-1} differences are most consistent for a source in the Toutle River vicinity, hinting that arrival #2 is displaced to the northwest of MSH. b) Map shows candidate source regions (MSH vent, Spirit Lake, and Toutle River drainage) and T_{RMS} contours. Enclosed contour is 3.0 s and contour intervals are 1.0 s.

[Moore and Rice, 1982]. The residual T_{RMS} reaches a minimum of ~2.6 s for an epicenter located ~9 km to the northwest of the volcano. We are reluctant to precisely pinpoint this source location because of the strong assumptions about the acoustic source as a point location and the atmospheric structure, which is simplistically modeled here as stratified and static since the eruption onset. Nevertheless, a dispersed region to the NW of MSH appears to be indicated by consistently low residuals (T_{RMS}<3.0) over a large region. We feel confident that this is evidence for a subsequent acoustic event occurring in the vicinity of Johnston Ridge, Coldwater Ridge, or the Toutle River drainage.

4. Discussion

The analyses of ground-coupled acoustic airwaves produced by MSH provide substantial constraints on its eruptive activity, but also present several important unresolved issues. We now focus briefly on two of the primary unresolved issues: The first is related to the eruptive chronology on the morning of May 18, 1980 and speculation about specific physical sources responsible for the multiple airwave observations (see Table 3). The second is a commentary on the suitability of ray theory for effective prediction of acoustic arrivals at regional distances.

4.1. Comments on eruptive chronology

Our data indicate that four or five distinct acoustic sources occur in the vicinity of MSH vent/conduit within 319 s of the original 8:32:11 PDT earthquake. These inferred source times and their relation to seismic events, and other observed eruptive chronology, are highlighted in a comparative timeline (Fig. 8).

Table 3
Summary of inferred event source times, elapsed times since earthquake, best fit travel time curves (from Fig. 3), and proposed source mechanisms as discussed in the text

Source time	Time (s) elapsed since 8:32:11 PDT	Arrivals	Source mechanism
8:32:21 PDT	10	#5	Initiation of landslide and initial unloading of cryptodome
8:34:05 PDT	114	#1/3/7	Shock produced by the 'second' explosion [19]
8:34:50 PDT	159	#8/6?	Additional eruptive pulse [22]
8:35:20 PDT	189	#9/6?	Additional eruptive pulse [22]
8:37:30 PDT	319	#2/4	Explosive event emanating from northern source region as hypothesized by Moore and Rice [27].

Relation to other observations are highlighted in the Fig. 8 timeline.

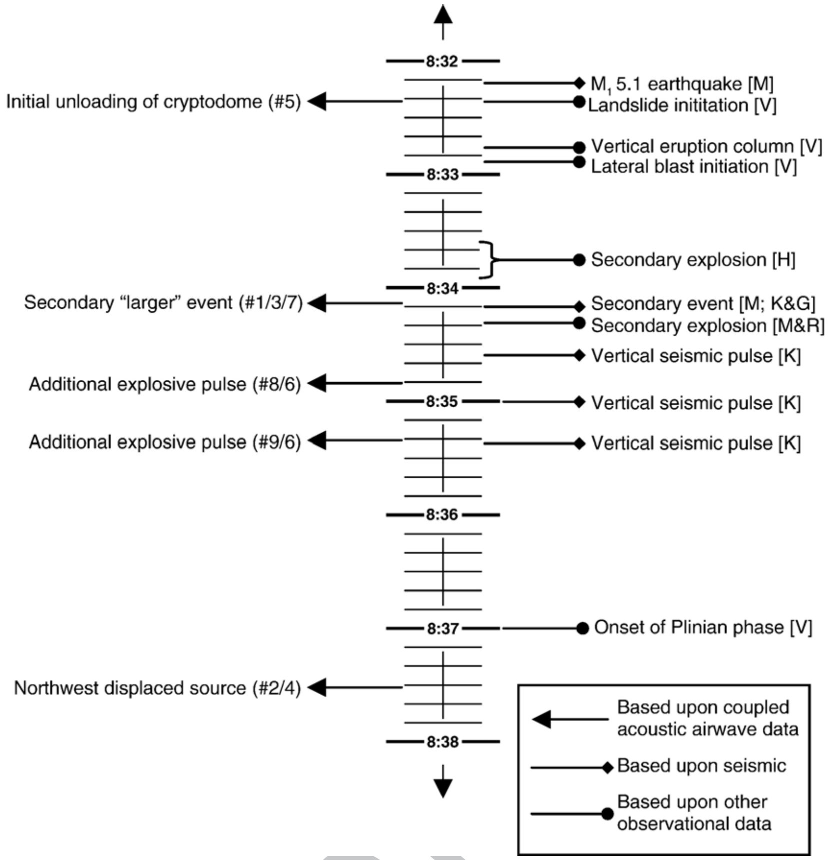

Fig. 8. Timeline chronology of inferred sources for seismo-acoustic events and other observations from: Malone et al. [26] [M], Voight [40] [V], Hoblitt [19] [H], Kanamori and Given [21] [K&G], Moore and Rice [27] [M&R], and Kanamori et al. [22] [K]. All times are PDT.

Based upon our transit time modeling, the occurrence of the first observed thermosphere refraction (arrival #5) coincides closely with the earthquake and/or landslide initiation. Time resolution of the forward ray-path modeling is such that an 8:32:11 PDT earthquake/landslide onset and subsequent 8:32:21 PDT cryptodome explosion event, as postulated by Brodsky et al. [6], would be virtually indistinguishable in our data. Although landslide and avalanche events are known to radiate substantial low frequency acoustic energy to regional distances (e.g., [35]), we suggest that explosive concussions would be a more natural mechanism for high-amplitude sound generation that also contains an audible component [29,34]. As such, we propose that the first identified acoustic source is likely an explosion (or series of explosions) occurring at ~8:32:21 PDT, which was induced by the mass movement unloading effect of the large landslide. The relatively sustained time duration of the ground-coupled airwaves for arrival #5 (see for example the ~25 s waveform from station EUK in the Fig. 2 inset) suggests a potential extended-duration source that is characteristic of an extended-duration sequence of explosive pulses. These explosive pulses might correspond to vertical seismic forces identified by Kanamori et al. [22] as the cyptodome is incrementally depressurized (refer to Fig. 1 in Brodsky et al. [6] for example).

The timing of the visible manifestation of the eruption onset, which includes a vertical plume rise at ~8:32:47 PDT and lateral blast initiation at ~8:32:56 PDT, is constrained by Voight [40] from the sequence of G. Rosenquist photos. However, we are unable to identify clear acoustic manifestation of these events as potential acoustic sources despite extensive transit time modeling under a range of conditions (utilizing May, June, and July profiles at 40° and 50° N). Variability in atmospheric structure and winds may account for propagation time uncertainties on the order of only a few tens of seconds (e.g., Fig. 5b), but these uncertainties are probably not sufficient to associate arrival #5 with the initial lateral blast. We largely discount the potential, and speculated, influence of supersonic transmission velocities, because even though the MSH airwaves might have originated as shock waves (i.e., [23,30]), reasonable shocks would decay to sonic speeds within a few kilometers of the source. It simply appears as though the initial explosive eruption occurring at 8:32:47–56 PDT was not energetic or impulsive enough to be responsible for the acoustic airwaves recorded by the PNSN network.

Following arrival #5, which we attribute to decompression-related explosive concussions, we hypothesize that the next source (8:34:05 PDT; arrivals #1/3/7) corresponds to a large explosive event from the vicinity of the depressurized conduit. According to Hoblitt [19] a large explosion followed the initial vertical column/lateral blast by 60–70 s, which would correspond to 8:33:47 to 8:33:57 PDT. Malone et al. [26] and Kanamori et al. [22] provide corroboration for the Hoblitt [19] source with seismic evidence for a second event occurring about 2 min after the initial 8:32:11 PDT earthquake. Such timing by both Hoblitt [19] and Malone et al. [26] coincides remarkably well with our inferred 8:34:05 PDT acoustic source. Seismic and remote sensing arguments are used by Hoblitt [19] to suggest that this second event was somewhat more powerful than prior event(s).

The second event of Hoblitt [19] corresponds well to the 8:34:05 PDT inferred acoustic source (arrivals #1/3/7), which may be conjoint with a seismically identified vertical thrust force identified by Kanamori et al. [22] and modeled by Brodsky et al. [6]. Although the timing of this vertical thrust is given a time of 8:34:35 (~30 s after the inferred source for arrivals #1/3/7), at least two smaller vertical thrust forces, occurring at 8:35:00 PDT and 8:35:22 PDT [6], exhibit timing that is very close to that of our stratosphere refracted arrivals #8 (8:34:50 PDT) and #9 (8:35:20 PDT). Several earlier vertical seismic thrusts identified by Kanamori et al. [22] at ~8:32:45, ~8:33:10, and ~8:33:45 PDT, are conspicuously absent in our data set and may be explained by poor coupling of these hypothesized events to the atmosphere.

We attribute at least two of the thermosphere refracted arrivals, including the large 8:34:05 source, to potential large explosive blasts. It is possible that one or both of these sources, or a combination of explosive pulses, may also be responsible for the acoustic-gravity phases, which were produced by MSH and observed worldwide [e.g., [3–5,7,32]]. For example, the microbarograph located 925 km from MSH at Berkely, CA recorded a wavetrain ~50 to 56 min after the 8:32:11 earthquake that includes two primary pulses of periods ~5 and ~6 min with amplitudes 350 and 220 Pa. These pulses were attributed to acoustic gravity waves generated by two distinct sources occurring approximately 6 min apart [5]. Though none of our ground-coupled arrivals provide explicit validation for two distinct energetic pulses separated by 6 min, it is notable that two sources (8:34:05 and 8:37:30 PDT; corresponding to arrivals #1/3 and #2/4) are especially prominent and are clearly recorded across most of the PNSN network (ranging from 151 to 341 km). These arrivals, separated by ~3.5 min, might be associated with the two significant pulses recorded at the Berkeley microbarograph, especially if the excitation of the second acoustic gravity wave was delayed relative to the first. We speculate that because gravity waves are generated by the injection of a large buoyant air mass (i.e., volcanic plume) into the atmosphere, a fast-rising column followed 3.5 min later (i.e., at 8:37:30 PDT) by a more slowly rising pulse could account for the timing discrepancy.

Eyewitness accounts may provide some limited constraints on the sequence of events at the very onset of the May 18 MSH eruption, although the visual observations of the volcano were largely obscured by ash and clouds shortly after ~8:33:00 PDT [33]. A couple of observers comment on being able to observe a shock wave, similar to that produced by a "nuclear explosion" that occurred "shortly after the initiation of a vertical eruption cloud." The timing of this event is uncertain and may or may not have been associated with a source of the recorded ground-coupled airwaves. An observer 17 km NE of the vent also reported seeing the horizontal blast (at ~8:32:56 PDT) and a shockwave "shortly following" the vertical eruption. This observer also cites "a clap of thunder" followed by a notable pressure change and is one of a very few people to report concussive noises within a few tens of kilometers of the volcano. Though exact timing is unclear, we speculate that this shock could be associated with an ~8:34:05 PDT origin (arrivals #1/3/7), which is considered here to be the 8:33:46–56 PDT event of Hoblitt [19]. In general, most first-hand audio reports within the zone of devastation primarily referred to 'rumbling' noises [33], but one observer 18 km north of MSH mentions three "rifle shots" at an unspecified time after the eruption, with an associated pressure change that "forced the observer to the ground." It is possible that these 'rifle shots' could also be associated with the 8:34:05 PDT event, or subsequent eruptive pulses inferred by Kanimori et al. [22]. It is also possible that many small shocks were produced during the first few minutes by the volcano and not propagated regionally.

At closer offsets National Weather Service barometers within Washington State recorded atmospheric perturbations associated with the eruption. The closest

Please cite this article as: J.B. Johnson, S.D. Malone, Ground-coupled acoustic airwaves from Mount St. Helens provide constraints on the May 18, 1980 eruption, Earth Planet. Sci. Lett. (2007), doi:10.1016/j.epsl.2007.03.001

barograph in Toledo, WA, 54 km from MSH, shows a 373 Pa spike followed after a short pause by a 13-minute 394 Pa decompression and then a second longer-duration compression. Reed [30] proposes that the decompression was associated with strong inflowing winds (towards the volcano) inducing a regional pressure low. In this scenario, inflowing winds are postulated to be a response to the MSH buoyant column rise. The secondary compression is hypothesized to result from mass injected into the atmosphere [30]. Unfortunately, the low temporal resolution afforded by the meteorological barometers inhibits the identification of relatively high-frequency energy that may be associated with near-infrasound (1 to 20 Hz) and/or sonic disturbances, which are the probable excitation mechanisms of the majority of our recorded ground-coupled recordings. In other words, multiple airwaves arriving in quick succession would be indistinguishable on the Toledo, WA long-period barometric records.

Many observers near to the volcano specifically reported strong inflowing winds headed towards the volcano about 5 min after the onset of the eruption. Several reports, from 25, 29, and 23 km N of the vent, comment on the northward-traveling blast cloud, which was suddenly “stood up” by vigorous winds (up to 80 miles per h) blowing south off Riffe Lake approximately 5 min after the eruption onset. The cloud was stood up NNW of the volcano and may coincide with observations of Moore and Rice [27], who claim that a cloud centered 12–14 km north of the volcano began to ascend at ~8:36:00. They speculate that the origin of this cloud may be the collision of a gas-charged dacitic cryptodome with Johnston Ridge/Toutle River drainage generating a significant ‘northern explosion,’ which was responsible for a 25 km high column displaced to the north of MSH [36].

Additional first-hand observations substantiate a displaced column to the north or northwest of the volcano. Photos taken by J. Christensen from near the summit of Mount Adams, 50 km E of MSH, clearly show the region around Spirit Lake and Coldwater Ridge were enveloped in a blast cloud and a convective cloud may be seen ascending in the north (see Fig. 9). In contrast, the region just to the south of the volcanic cone is entirely clear at this time. These observations have led to speculation that a hot portion of the MSH cryptodome

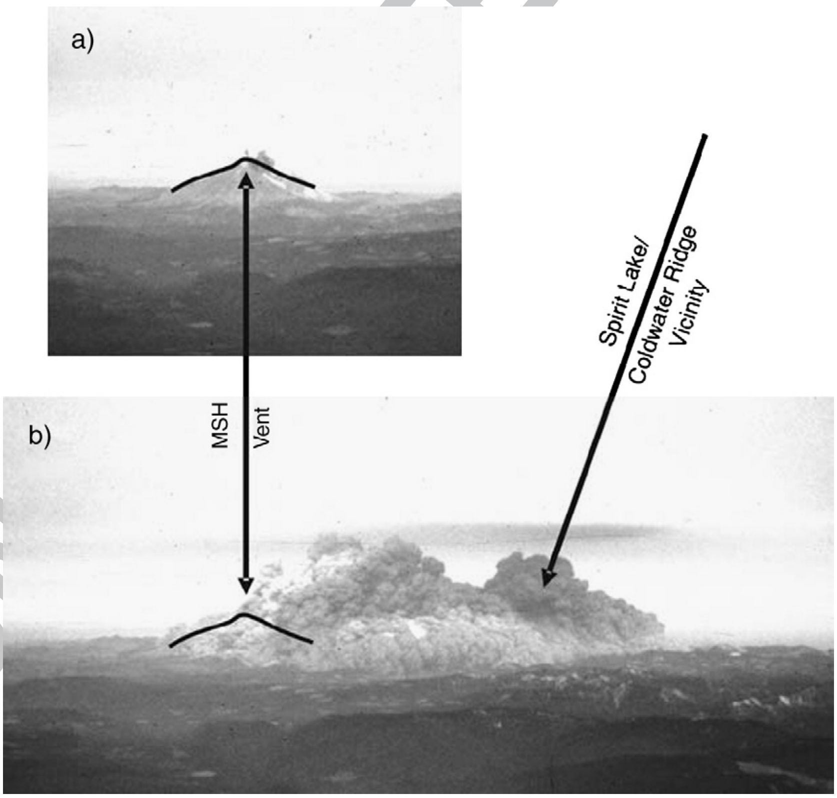

Fig. 9. Photos taken from Mount Adams (~53 km to the East) by J. Christensen taken: a) shortly after the onset of the ~8:32:47 PDT vertical plume, and b) approximately 3 to 5 min later. Horizontal expanse of the cloud in the second image is ~14 km south to north.

Please cite this article as: J.B. Johnson, S.D. Malone, Ground-coupled acoustic airwaves from Mount St. Helens provide constraints on the May 18, 1980 eruption, Earth Planet. Sci. Lett. (2007), doi:10.1016/j.epsl.2007.03.001

could have slid into Spirit Lake and generated a significant (and time-delayed) phreatic blast from this vicinity [[27] and unreferenced information posted at http://www.answers.com/topic/1980-eruption-of-mount-st-helens]. Others, including Hoblitt [19], conclude that this 'northern explosion' may have resulted from interaction of the pyroclastic density flow with rough topography in the Toutle River drainage, initiating a buoyant ash cloud. The study here of the acoustic airwaves, and specifically of arrival #2, supports a secondary northern source that is located substantially to the west of Spirit Lake (Fig. 7). Based upon our acoustic evidence, we maintain the possibility of a displaced 'northwest source' in the vicinity of Toutle River Drainage and/or Johnston Ridge that is unassociated with a postulated Spirit Lake event.

4.2. Comments on suitability of ray tracing

Observational data coupled with forward ray tracing indicate MSH acoustic refraction from high velocity regions in both the stratosphere and thermosphere. Although sound absorption in the thermosphere can be severe [e.g., [37]], this study along with those of others provides evidence that acoustic perturbations can return to earth from altitudes well above 100 km [e.g., [25,13]].

Although the ray tracing performed in this study is able to generally reproduce the PNSN-recorded arrival times, it is less effective at predicting arrivals closer than 200 km from MSH. For instance, arrivals #1/2 include 9 stations that lie within the predicted acoustic shadow zone. It is clear that arrivals #1/2 do not represent stratospheric refractions because their apparent velocities (501 and 520 m/s) are far too fast, but they do strongly suggest rays turning in the high velocity thermosphere, well above 120 km. If this energy is in fact reaching the thermosphere, the problem is that ray theory does not satisfactorily predict acoustic energy returning to earth at such close offsets. We are unable to model these near-offset 'thermosphere refractions' despite attempts to force extreme (post-eruption) changes to the atmospheric velocity structure in the vicinity of MSH.

Thermosphere winds are the least well-constrained parameters in our forward ray path modeling and may offer one potential explanation for the observation of near-offset thermosphere refractions. Thermosphere winds are affected by solar activity and vary according to location, season, and most significantly to time of day [18]. Because we have no empirical measurements of thermosphere winds for the morning of May 18, we modeled acoustic radiation for a dramatic range of conceivable wind velocities. Hedin et al. [18] indicate that longitudinally averaged annual zonal winds can vary from ∼−130 m/s to ∼+90 m/s at 6:00 AM and 6:00 PM respectively at 45° N latitude. We thus attempted to model travel time curves for exceptional wind conditions (+/−150 m/s) above 120 kilometer altitude. We found that extreme winds in the thermosphere in the direction of acoustic propagation do facilitate downward refraction, however they only succeed in bringing the nearest offset to about 170 km. It is still puzzling, and observationally significant, that we see apparent thermosphere refracted energy closer than 120 km for both zonal and meridional propagation. We conclude that classical ray theory may be deficient at predicting arrivals at these close offsets. The MSH data appear to provide evidence for the prevalence of leaky atmospheric waveguides and/or the importance of dispersion and scattering during regional sound propagation (e.g., [8]).

One last unresolved issue is related to the two ground-coupled airwaves recorded at the seismic station LON only 67 km from the MSH vent. Based upon the time difference between the two observed arrivals at LON (177 s; Table 2), it would appear as though the sources responsible for the LON arrivals are conjoint with the sources responsible for arrivals #5/6 originating at ∼8:32:21 and ∼8:35:20 PDT. However, if we assume that the initial uncorking of MSH is responsible for the 8:47:50 PDT arrival at LON, this would imply a net transit time of ∼15 min (∼900 s) for a horizontal propagation distance of only 67 km (i.e., a straight-line velocity of 74 m/s). For this arrival to be an acoustic wave (with average velocity in excess of 300 m/s), the propagation path would need to be ∼300 km and thus require an effective 'reflection' in the thermosphere at an altitude of 150 km. Because internal atmospheric sound reflections are not considered plausible, we conclude that the LON arrival(s) can not be caused by ground-coupled acoustic waves. Rather, the picked arrivals may reflect mass transport of the atmosphere due to abrupt regional barometric changes and potential associated winds. The LON ground-coupled seismic deflections could be associated with phenomena that were documented by Rosenbaum and Waitt [33] and that might have been induced by the massive buoyant column rise [30].

5. Summary

Throughout Washington State, both people and seismometers 'heard' the paroxysmal eruption of MSH on the morning of May 18, 1980. Data corresponding to ground-coupled airwaves substantiate that the first

Please cite this article as: J.B. Johnson, S.D. Malone, Ground-coupled acoustic airwaves from Mount St. Helens provide constraints on the May 18, 1980 eruption, Earth Planet. Sci. Lett. (2007), doi:10.1016/j.epsl.2007.03.001

5 min of the eruption was complicated with multiple discrete events occurring during this time. Although the first 'acoustic event' likely corresponded to uncorking of the cryptodome following the initial landslide onset, subsequent events may be associated with other potentially diverse phenomena, such as the onset of vertical and lateral explosive pulses from the central vent, and convective plume rise originating from the northwest of the MSH edifice due to hot debris avalanche and/or cryptodome slamming into the Toutle River drainage. This displaced northwest source is substantiated by acoustic arrival time residuals recorded across the network of PNSN seismometers.

Perturbations of the atmosphere during the MSH eruption produced high-intensity acoustic waves, both low-frequency and audible, which were heard by humans and simultaneously recorded by seismometers. Based upon acoustic arrival times across the PNSN seismic network we infer that much of this energy radiated into the stratosphere and thermosphere before refracting back to earth. Scattering of the acoustic energy facilitated acoustic energy returning to earth at a greater range of offsets than would generally be expected with ray theory. Nevertheless, a significant shadow zone (region of inaudibility) was preserved within a few tens of kilometers of the volcano. This shadow zone, which was noted by the general public, and has been similarly observed at other erupting volcanoes, is most easily attributed to the upward refraction of acoustic airwaves in a temperature stratified atmosphere.

Acknowledgments

We thank M. Garces and two anonymous reviewers for the helpful input. This work was supported by the US Geological Survey Cooperative agreement (04HQA005 and 1434-HQ-98-AG-01937) for the operation of the Pacific Northwest Seismograph Network (PNSN) and by NSF EAR #0440225.

References

[1] K. Aki, R. Richards, Quantitative Seismology: Theory and Methods, W.H. Freeman, San Francisco, 1980 932 pp.
[2] W.E. Baker, Explosions in Air, University of Texas Press, Austin, 1973 268 pp.
[3] J.R. Banister, Pressure wave generated by the Mount St. Helens eruption, J. Geophys. Res. 89 (D3) (1984) 4895–4904.
[4] M. Bath, Atmospheric waves from Mount St. Helens, EOS Trans. AGU 63 (1982) 193.
[5] B.A. Bolt, T. Tanimoto, Atmospheric oscillations after the May 18, 1980 eruption of Mount St. Helens, EOS Trans. AGU 62 (1981) 529–530.
[6] E.E. Brodsky, H. Kanamori, B. Sturtevant, A seismically constrained mass discharge rate for the initiation of the May 18, 1980 Mount St. Helens eruption, J. Geophys. Res. 104 (B12) (1999) 29387–29400.
[7] W.L. Donn, N.K. Balachandran, Mount St. Helens eruption of 18 May, 1980: air waves and explosive yield, Science 213 (1981) 539–541.
[8] D.P. Drob, J.M. Picone, M. Garces, Global morphology of infrasound propagation, J. Geophys. Res. 108 (D21) (2003) (4680), doi:10.1029/2002JD003307.
[9] C. Fairfield, OMSI sound project, the acoustic effects of the Mount St. Helens eruption on May 18, 1980, Or. Geol. 42 (12) (1980) 200–202.
[10] E.L. Fleming, S. Chandra, M.R. Shoeberl, J.J. Barnett, Monthly mean global climatology of temperature, wind, geopotential height and pressure for 0–120 km, Nataional Aeronautics and Space Administration 100697, Washington D.C., 1988.
[11] R.D. Ford, Introduction to Acoustics, Elsevier, New York, 1970 154 pp.
[12] M.A. Garces, M.T. Hagerty, S.Y. Schwartz, Magma acoustics and time-varying melt properties at Arenal Volcano, Costa Rica, Geophys. Res. Lett. 25 (13) (1998) 2293–2296.
[13] M.A. Garces, M. Willis, C. Hetzer, A. Le Pichon, D. Drob, On using ocean swells for continuous infrasonic measurements of winds and temperature in the lower, middle, and upper atmosphere, Geophys. Res. Lett. 31 (L19304) (2004), doi:10.1029/2004L020696.
[14] T.M. Georges, A program for calculating 3-D acoustic-gravity ray paths in the atmosphere, Tech. Rep. ERL 212-WPL-16, Natl. Oceanic and Atmos. Admin., Boulder, CO, 1971.
[15] T.M. Georges, W.H. Beasley, Refraction of infrasound by upper-atmospheric winds, J. Acoust. Soc. Am. 61 (1) (1977) 28–34.
[16] A.E. Hedin, MSIS-86 thermospheric model, J. Geophys. Res. 92 (A5) (1987) 4649–4662.
[17] A.E. Hedin, Extension of the MSIS thermosphere model into the middle and lower atmosphere, J. Geophys. Res. 96 (A2) (1991) 1159–1172.
[18] A.E. Hedin, M.A. Biondi, R.G. Burnside, R.M. Johnson, T.L. Killeen, C. Mazaudier, J.W. Meriwether, R.J. Sica, R.W. Smith, N.W. Spencer, V.B. Wickwar, T.S. Virdi, Revised global model of thermosphere winds using satellite and ground-based observations, J. Geophys. Res. 96 (A5) (1991) 7657–7688.
[19] R.P. Hoblitt, Was the 18 May 1980 lateral blast at Mt St Helens the product of two explosions? Philos. Trans. R. Soc. Lond., A 35 (2000) 1639–1661.
[20] R.E. Holasek, S. Self, GOES weather satellite observations and measurements of the May 18, 1980, Mount St. Helens eruption, J. Geophys. Res. 100 (B5) (1995) 8469–8487.
[21] H. Kanamori, J.W. Given, Analysis of long-period seismic waves excited by the May 18, 1980 eruption of Mount St. Helens: a terrestrial monopole? J. Geophys. Res. 87 (B7) (1982) 5422–5432.
[22] H. Kanamori, J.W. Given, T. Lay, Analysis of seismic body waves excited by the Mount St. Helens eruption of May 18, 1980, J. Geophys. Res. 89 (1856–1866) (1984).
[23] Kieffer, Time scale for the first moments of the May 18 eruption, in: P.W. Lipman, D.R. Mullineaux (Eds.), The 1980 Eruptions of Mount St. Helens, Washington, U.S. Geological Survey Professional Paper, 1981.
[24] I.O. Kitov, O.P. Murphy, O.P. Kusnetsov, B.W. Barker, N.I. Nedoshivin, An analysis of seismic and acoustic signals

measured from a series of atmospheric and near-surface explosions, Bull. Seismol. Soc. Am. 87 (6) (1997) 1553–1562.

[25] A. Le Pichon, M. Garces, E. Blanc, M. Barthelemy, D. Drob, Acoustic propagation and atmosphere characteristics derived from infrasonic waves generated by the Concorde, J. Acoust. Soc. Am. 111 (2002) 629–641.

[26] S.D. Malone, E.T. Endo, C.S. Weaver, J.W. Ramey, Seismic monitoring for eruption prediction, in: P.W. Lipman, D.R. Mullineaux (Eds.), The 1980 Eruptions of Mount St. Helens, Washington, U.S. Geological Survey Professional Paper, vol. 1250, 1981, pp. 803–813.

[27] J.G. Moore, C.J. Rice, Chronology and character of the May 18, 1980, explosive eruptions of Mount St. Helens, Explosive volcanism: inception, evolution, and hazards, National Academy Press, Washington D.C., 1984, pp. 133–142.

[28] J. Power, Sounds during the August 18, 1992, Spurr Eruption, Alaska Volcano Observatory Newsletter, vol. 5, 1993, pp. 14–15.

[29] R. Raspet, Shock waves, blast waves, and sonic booms, in: M. Crocker (Ed.), Handbook of Acoustics, John Wiley & Sons, New York, 1998, pp. 293–303.

[30] J.W. Reed, Air pressure waves from Mount St. Helens eruptions, J. Geophys. Res. 92 (D10) (1987) 11979–11982.

[31] D.E. Rees, CIRA 1986: part I thermospheric models, Adv. Space Res. 8 (5–6) (1986).

[32] A.R. Ritsema, Observations of Mount St. Helens eruption, EOS Trans. AGU 61 (1980) 1201–1202.

[33] J.G. Rosenbaum, R.B.J. Waitt, Summary of eyewitness accounts of the May 18 eruption, in: P.W. Lipman, D.R. Mullineaux (Eds.), The 1980 Eruptions of Mount St. Helens, Washington, U.S. Geological Survey Professional Paper, vol. 1250, 1981, pp. 53–68.

[34] C.A. Rowe, R.C. Aster, P.R. Kyle, R.R. Dibble, J.W. Schlue, Seismic and acoustic observations at Mount Erebus Volcano, Ross Island, Antarctica, J. Volcanol. Geotherm. Res. 101 (1–2) (2000) 105–128.

[35] E. Scott, C. Hayward, Avalanche-generated infrasound signals, EOS Trans. AGU, Fall Meet. Suppl. 84 (46) (2003) (U31B-0008).

[36] R.S.J. Sparks, J.G. Moore, C.J. Rice, The initial giant umbrella cloud of the May 18th, 1980, explosive eruption of Mount St. Helens, J. Volcanol. Geotherm. Res 28 (3–4) (1986) 257–274.

[37] L.C. Sutherland, H.E. Bass, Atmospheric absorption in the atmosphere up to 160 km, J. Acoust. Soc. Am. 115 (3) (2003) 1012–1032.

[38] G. Symons, The Eruption of Krakatau and Subsequent Phenomena, Trubner & Co., London, 1888.

[39] M. Tahira, M. Nomura, Y. Sawada, K. Kamo, Infrasonic and acoustic-gravity waves generated by the Mount Pinatubo eruption of June 15, 1991, in: C.G. Newhall, R.S. Punongbayan (Eds.), Fire and Mud, University of Washington Press, Seattle, 1996, pp. 601–614.

[40] B. Voight, Time scale for the first moments of the May 18 eruption, in: P.W. Lipman, D.R. Mullineaux (Eds.), The 1980 Eruptions of Mount St. Helens, Washington, U.S. Geological Survey Professional Paper, vol. 1250, 1981, pp. 69–92.